

ORIGINAL ARTICLE

Using Updated and Expanded Data to Estimate the Unmeasured Rotational Data of a Bolted Structure

I.I Wan Iskandar Mirza¹, A. Kyprianou², M.N Abdul Rani^{1*}, M.A Yunus¹ and R. Febrina³¹Structural Dynamics Analysis & Validation (SDAV), College of Engineering, Universiti Teknologi MARA (UiTM), 40450 Shah Alam, Selangor, Malaysia²Department of Mechanical and Manufacturing Engineering, University of Cyprus, 2112 Cyprus³Department of Civil Engineering, Malahayati University, 35153 Lampung, Indonesia

ABSTRACT – For frequency-based substructuring (FBS) to be accurate, translational and rotational data must be available at the connection points between substructures. However, obtaining rotational FRFs from experimental modal analyses is very difficult in practice. In this paper, an alternative method for estimating rotational FRFs is proposed using an approximated simplified finite element model (ASFE), modal updating, and mode expansion. The proposed approach was demonstrated on an assembled structure consisting of an irregular plate (test model) and a simple beam (FE model). The SEREP method was used to augment the translational and rotational FRFs to the updated ASFE mode shapes. The expanded rotational FRF of the test model was validated with the measured rotational FRF obtained from a piezoelectric direct rotational accelerometer. The results showed that the proposed approach for FBS correctly predicted the experimental FRF of the assembled structure with 90% accuracy. The FBS method is no longer dependent on the experimental rotational FRF, which is very difficult to measure with the methodology presented here.

ARTICLE HISTORYReceived: 7th Oct 2021Revised: 17th Feb 2022Accepted: 17th Mar 2022**KEYWORDS***Rotational FRF;**Model updating;**FRAC;**Mode expansion*

INTRODUCTION

Frequency-based substructuring (FBS) [1]- [3] can be used to accurately predict composite engineering structures. However, it should be noted that the FBS method depends heavily on the coupling interface to accurately predict the dynamic behaviour. The coupling interface is sensitive to translational and rotational frequency response functions (FRFs), the latter being very difficult to determine experimentally. It is well known that the rotational FRFs at the interfaces are essential for the accurate prediction of the FRFs of the assembled structure [4], [5]. This is because the rotational FRFs account for 75% of the FRF matrix of a single node. This means that neglecting the rotational FRFs seriously affects the accuracy of the interface flexibility of the test model and leads to erroneous coupling results. In FBS, the main challenge is to identify the rotational FRFs that are critical to the accuracy of the method in predicting and calculating the vibration behaviour of the assembled structure [6].

Over the years, various methods for estimating rotational FRFs have been proposed [7], [8]. For example, researchers [9], [10] have used two accelerometers with the same sensitivity to estimate rotational FRF. Methods using T-block [11] and X-block [12] have proven successful in structural modification applications. In particular, the X-block basis method used for structural modification of a helicopter cone proved to be more effective as it used several translational accelerometers to estimate multiple rotational FRFs. Although the X-block method is an effective method for estimating rotational FRFs, it has two disadvantages concerning its applicability and complexity. The disadvantage that limits the applicability of the method is that the test structure must be significantly larger and heavier than the X-block. The complexity arises from the fact that the process of estimating the rotational FRFs must incorporate the dynamics of the X-block.

With the advent of technology and the development of rotational accelerometers, the rotational FRFs of a test structure can be effectively and directly measured [13], [14]. The rotational accelerometer can only be used to measure the rotational data of force excitations. This is because the current state of the art does not provide a method for pure moment excitation [15]. As a consequence of this limitation, semi-analytical or computational methods must be developed to determine the full FRF matrix. In this context, many methods have been proposed, most of which use the concept of mode expansion. The accuracy of mode expansion techniques depends mainly on the accuracy of the FE model of the structure under study. The finite elements developed for complicated structures are usually inaccurate, resulting in an inaccurate estimate of the rotational FRFs.

This study presents a new scheme for estimating rotational FRFs using a simplified and approximated finite element model (ASFE), the modal updating method and the mode expansion method. The process flow for obtaining rotational FRFs is shown in Figure 1. An assembled structure consisting of two substructures: an irregular plate and a beam, as shown in Figure 2 [16], illustrates the proposed methodology. The two substructures are joined by two connection points.

The proposed approach is used to develop the expanded ASFE model of the irregular plate, which includes translation and rotational data, and is then used in the FBS method to predict the obtained experimental FRF of the assembled structure.

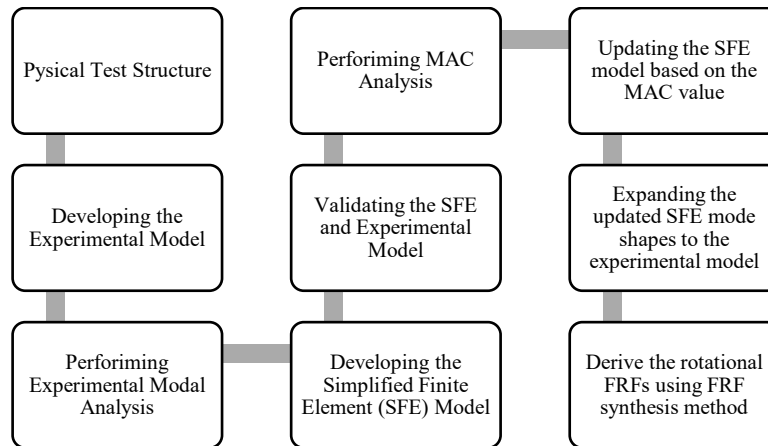


Figure 1. Process flow for obtaining rotational FRFs.

METHODOLOGY

This study focuses on the frequency range between 0Hz and 1500Hz, acquiring several resonance peaks. The frequency of interest of 0-1500Hz was chosen to avoid truncation of the FRF calculated. Note that the FRF of the substructure should be at least 1.5 greater than that of the assembled structure during FRF coupling. The reference point used in this study is connection point 1. The FRF at the reference point of the assembled test structure was measured by the impact testing method to validate the FBS obtained by the proposed method. Details of the experimental setup and the measured FRF of the assembled structure can be found in [16]. After measuring the FRF at connection point 1, the structure was disassembled for FRF analysis of the individual substructures. The FE model of the beam was created with HEXA elements (3D element type). The FRFs of the beam were calculated using the modal frequency response method. The translational FRFs of the irregular plate were measured directly, and its rotational FRFs were expanded from the approximated and simplified FE (ASFE) model. The details are explained in the following subsection.

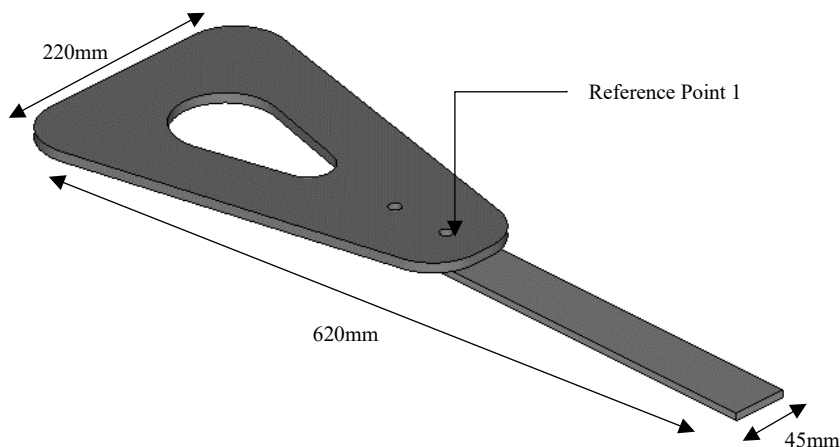


Figure 2. The assembled test structure.

The Development of the Approximated and Simplified Finite Element (ASFE) Model

Modal expansion methods depend primarily on the accuracy of the FE models. In some cases involving complex structures, developing accurate FE models is a very challenging and time-consuming activity. As an alternative to developing detailed FE models, a simplified and approximate modelling approach was used to build the FE model of the irregular plate. In this work, the ASFE model of the irregular plate was modelled by using shell elements based on the simplified geometry of the model as shown in Figure. 3. The simplified geometry was then discretised into 12 QUAD4 and 6 TRIA3 elements. The methodology for developing the ASFE model can be found in [16].

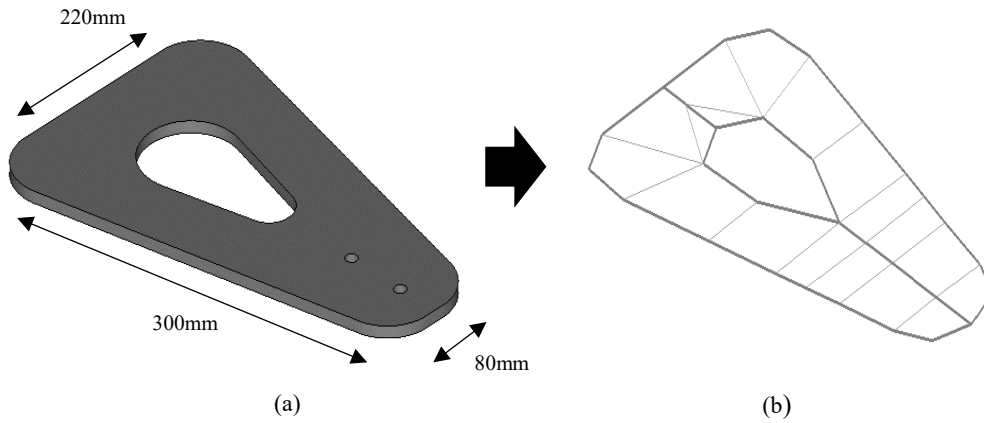


Figure 3. (a) Test and (b) ASFE model of the irregular plate.

EMA of the irregular plate

Experimental modal analysis (EMA) was performed on the irregular plate to measure the natural frequencies and mode shapes used in model updating [17]. The EMA was performed by suspending the irregular plate with two soft suspensions to simulate free-free conditions [18], [19]. The details of the experimental setup for the irregular plate can be found in [16]. In this work, the Kistler 8840, as shown in Figure 4, was used to measure the rotational FRF. This sensor is made of a very stable quartz crystal, and the accelerometer can be operated with a 20-30 VDC power supply. The technical data of the Kistler 8840 can be found in [13], [15] and are listed in Table 1. In this work, only the rotational FRF of the force excitation was recorded.

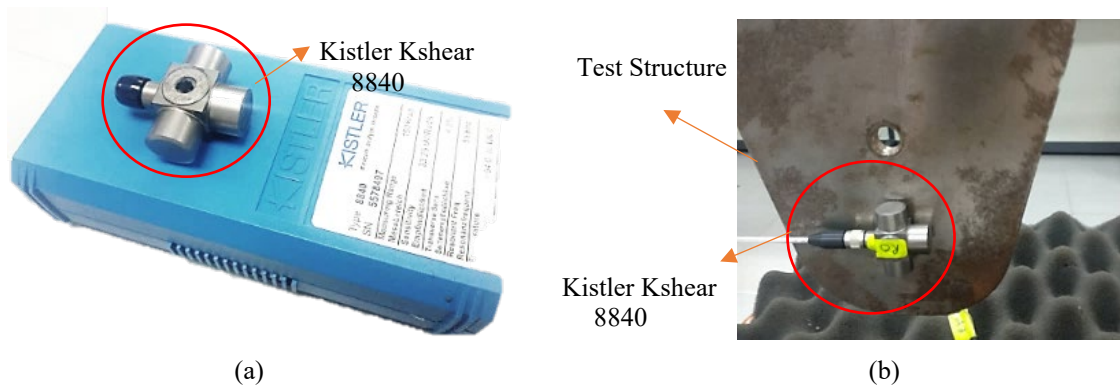


Figure 4. (a) Kistler 8840 rotational accelerometer and (b) mounting configuration.

Table 1. Kistler Kshear 8840 specification.

Specification	Value
Sensitivity	35 μV/rad/s
Frequency response, ±10%	0 – 2000 Hz
Acceleration range	±150 krad/s ²
Maximum limit	±200 krad/s ²
Source voltage	20-30 V
Source current	4 mA

Updating the ASFE Model

In ASFE updating, certain parameters are systematically adjusted based on experimental data. This process is mainly carried out to improve the accuracy of the ASFE model [20]. ASFE parameters that are sensitive to experimental data are identified through sensitivity analysis. Since in this study, the experimental data are in the form of mode shapes Φ and natural frequencies ω , the sensitivity of the parameters θ is determined by the matrix S given by,

$$S = \Phi_i^T \left[\frac{\delta K}{\delta \theta_j} - \omega_i \frac{\delta M}{\delta \theta_j} \right] \Phi_i \tag{1}$$

The subscript i and j indicate the i -th eigenvalue and the j -th parameter [21], [22]. The following four parameters were subjected to updating in this study: Density, thickness, Young's modulus and Poisson's ratio.

The proposed scheme involves mode expansion and synthesis to ensure that these processes yield accurate results meaning that the updated eigenvectors must be very close to their experimental counterparts. Consequently, the modal assurance criterion (MAC) [15], which quantifies the similarity between two mode shapes, was selected as the fitness function for the updating process. The degree of similarity between the mode shapes of the ASFE and the experimental ones is quantified using MAC defined by [23],

$$MAC(\phi_{ASFE}, \phi_{EXP}) = \frac{|\phi_{ASFE}^T \phi_{EXP}|^2}{(\phi_{ASFE}^T \phi_{ASFE})(\phi_{EXP}^T \phi_{EXP})} \times 100\% \tag{2}$$

where ϕ_{ASFE} and ϕ_{EXP} are ASFE and EMA modal vectors, respectively. The MAC values can be cast in an $n \times m$ matrix, where n is the number of ASFE mode shapes and m is the number of EMA mode shapes. In this study, seven mode shapes were employed in the modal updating carried out using MSC NASTRAN Software. Figure 5(a) and 5(b) present the initial, Figure 5(a) and updated, Figure 5(b) MAC values between the ASFE and experimental mode shapes. The MAC values along the diagonal must be close to 100% (approaching the red colour in Figure 5(a) and (b)) and express the similarity of the EMA and FE mode shapes.

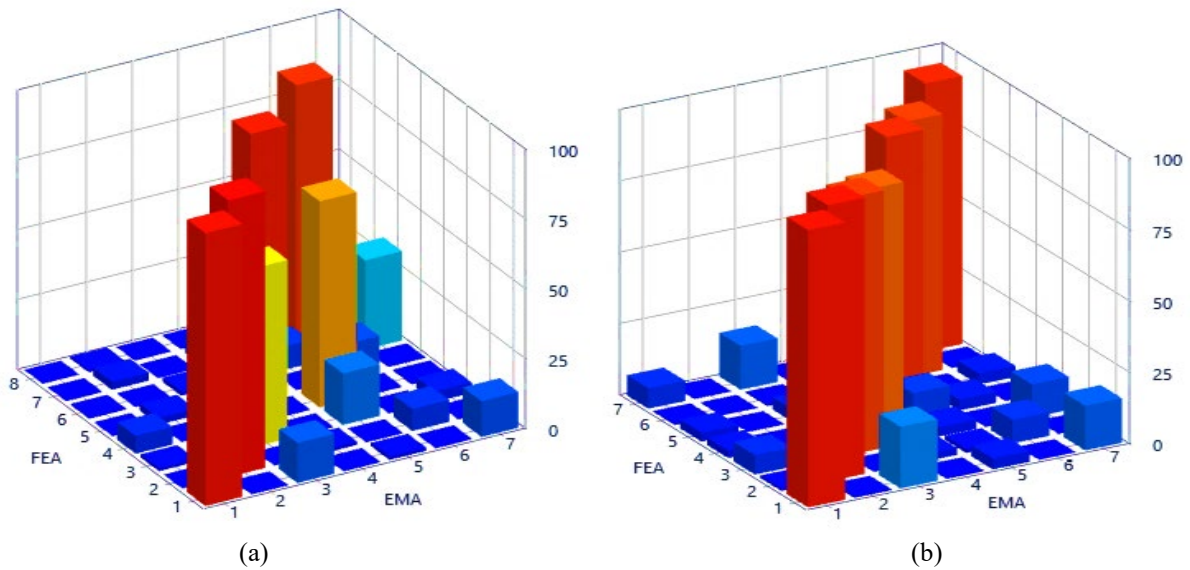


Figure 5. 3D view of MAC for (a) the Initial ASFE and (b) the updated ASFE.

Figure 5(a) shows that the calculated MAC values indicate that the initial ASFE model is not in good agreement with the test model. The MAC values along the diagonal indicate that the mode shapes of the initial ASFE model are not well correlated with the experimental ones. The observed low MAC values are due to the material properties and the dimensions used in developing the ASFE model. However, the updating improved the MAC values significantly, as depicted in Figure 5(b). Due to this improvement, the updated ASFE model is on the one hand suitable to represent the dynamic behaviour of the irregular plate and to perform the mode expansion.

Expanding the ASFE Model

The mode expansion objective of the updated ASFE model of the irregular plate is to acquire the rotational DOFs that are not measured. The system equivalent reduction expansion procedure (SEREP) [14] was used in this study to expand the unmeasured rotational data from the improved ASFE model of the irregular plate. The SEREP procedure was performed based on the mode shapes of the updated ASFE model. The expanded modal vector with a full set of DOFs, ϕ_n is expressed in the form of:

$$\phi_n = \begin{bmatrix} \phi_{ASFE} \\ \phi_{EXP} \end{bmatrix} = \mathbf{T}_{SEREP} \phi_{ASFE} \tag{3}$$

where

$$\mathbf{T}_{SEREP} = \begin{bmatrix} \phi_{ASFE} \\ \phi_{EXP} \end{bmatrix} \phi_{ASFE}^g \tag{4}$$

so the expanded mode shapes are;

$$\phi_n = \begin{bmatrix} \phi_{ASFE} \\ \phi_{EXP} \end{bmatrix} \phi_{ASFE}^g \phi_{EXP} \tag{5}$$

where ϕ_{EXP} , ϕ_{ASFE} and T_{SEREP} are EMA modal vectors, updated ASFE modal vectors and SEREP transformation matrices. The natural frequencies of the expanded model were preserved based on the original natural frequencies obtained from the EMA.

The improved model, henceforth referred to as the expanded ASFE model, is then used to calculate the rotational FRF using the FRF synthesis technique. The technique for synthesising the FRF is described in detail in [23]. In this method, the synthesised FRF matrix $H_{exp}(\omega_k)$ of the expanded model and the mode shapes ϕ are represented as follows:

$$H_{exp}(\omega_k) = \sum_{i=1}^N \frac{\{\phi\}_i \{\phi\}_i^T}{(\omega_{n_i}^2 - \omega_k^2) + j2\xi_i \omega_k \omega_{n_i}} \tag{6}$$

where N represents the number of modes, $\{\phi\}_i$ represents the i th expanded mode shapes, ω_{n_i} represents i th natural frequency and ξ_i represents the i th modal damping ratio. The translational and rotational FRFs obtained using the expanded ASFE model were validated by comparing them with the experimental FRFs. For comparison purposes, overlay plots of the experimental and synthesised FRFs are shown in Figures 6 and 7. Figure 6 presents the translational FRFs, while Figure 7 shows the rotational FRFs. Both FRFs were obtained by the translational and rotational response of the reference point to the force excitation.

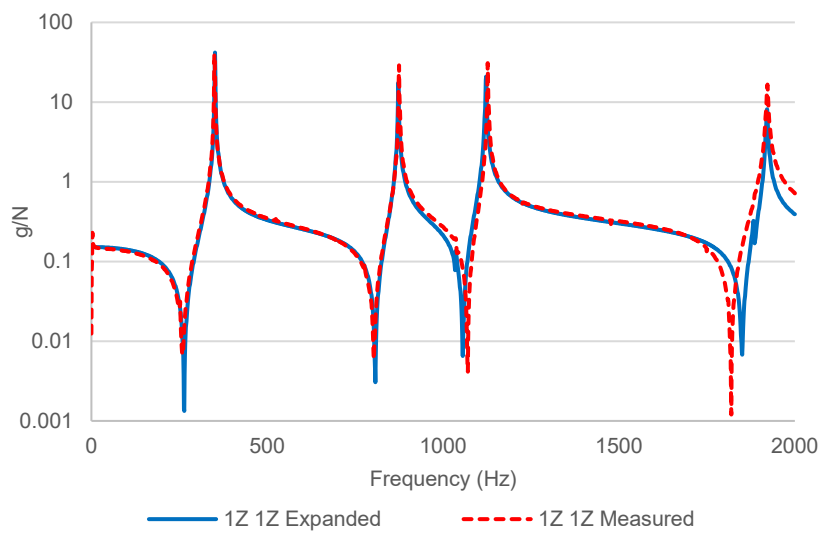


Figure 6. The evaluation of translational FRF between the test and expanded ASFE model at the reference point.

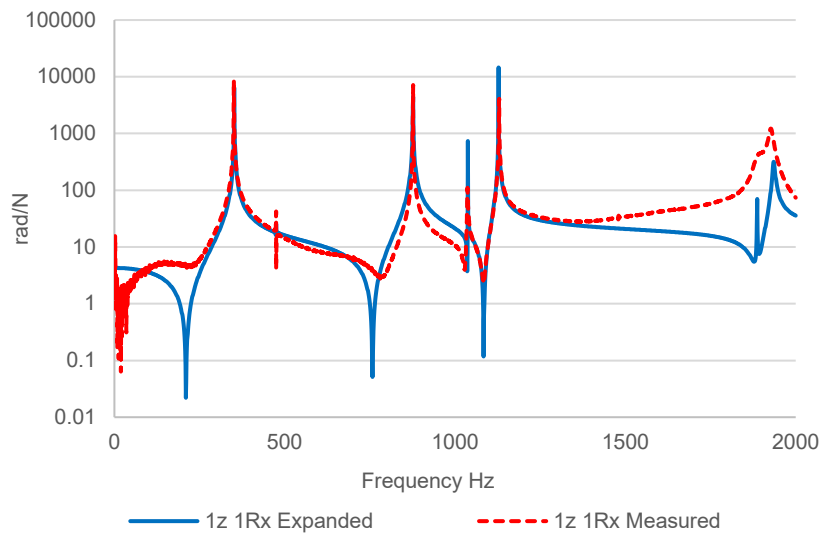


Figure 7. The evaluation of force-excitation rotational FRF between the and expanded ASFE model at the reference point.

Figure 6 and Figure 7 show that all the resonance peaks of the expanded FRF data obtained with the expanded ASFE model agree well with the peaks of the experimental FRFs. On the other hand, the expanded FRFs from both figures show

slight discrepancies in the anti-resonance peaks, especially in the frequency range between 1800-2000 Hz. These differences are due to the fact that the synthesised FRFs do not take into account the effect of the out-of-range modes.

In this study, the Frequency Response Assurance Criteria (FRAC) was used to quantify the degree of similarity between the expanded and measured FRFs. The main objective of comparing the FRFs is to evaluate the accuracy of the expanded FRFs over the frequency range in question using a representative percentage value. A detailed explanation of the FRAC analysis can be found in [24].

The degree of similarity between the expanded translational FRF and its measured counterpart is 96.78%, while the expanded force-excitation-rotational FRF has a similarity of 90.81% with the measured one. The degree of similarity for both derived FRFs is well above 70%, which is an acceptable value [24]. It is therefore essential to note that the FRFs calculated with the expanded ASFE model are very similar to the measured FRFs of the irregular plate.

RESULTS AND DISCUSSION

In the previous section, the accuracy of the force-excitation rotational FRF of the expanded ASFE model of the irregular plate was discussed. However, the moment-excitation rotational FRF cannot be validated using the same procedure that was used for the force excitation rotational FRF. This is because measuring the moment-excitation rotational FRFs is exceptionally challenging. There are many shortcomings in solving the problem, such as the inability to introduce and control moment- excitations in experiments, the insufficient understanding of the measurement process and the unavailability of moment measurement sensors.

The FBS technique is used to validate the accuracy of the moment-excitation rotational FRF produced from the enlarged ASFE. [18] covers a comprehensive and mathematical description of the FBS technique. It is worth emphasising that the accuracy of the expanded ASFE model will be acceptable if the coupled FRF calculated from the expanded ASFE model is similar to the measured counterparts. To test the proposed approach, the FBS method was performed in this study by coupling the FRFs obtained from the expanded ASFE model with the beam's FE model of the beam. The FRF of the FBS using the expanded ASFE model was compared with the measured FRF of the assembled structure and the proposed model of [16], in which an updated SFE model is used in the FBS method.

An interesting observation from the comparison of the FRF between the FBS using the expanded ASFE model and the FBS using the updated SFE model is that the FBS using the updated SFE model does not match the modes occurring at high frequencies (in Figure 8). In contrast, the FBS using the expanded ASFE model performs much better at higher frequencies, Figure 10. Figure 8 shows that the FBS can accurately predict the coupled FRF of the assembled structure using the updated SFE model. However, the prediction model seems to be accurate only for predicting modes in the frequency range of 0 to 700 Hz and is not able to capture higher modes with reasonable accuracy (in Figure 9). Furthermore, there is no strong correlation between the test and the improved SFE model, as shown by the FRAC value of 30.47 per cent. As a result, the improved SFE model is not accurate enough to correctly predict the rotational FRF of the irregular plate.

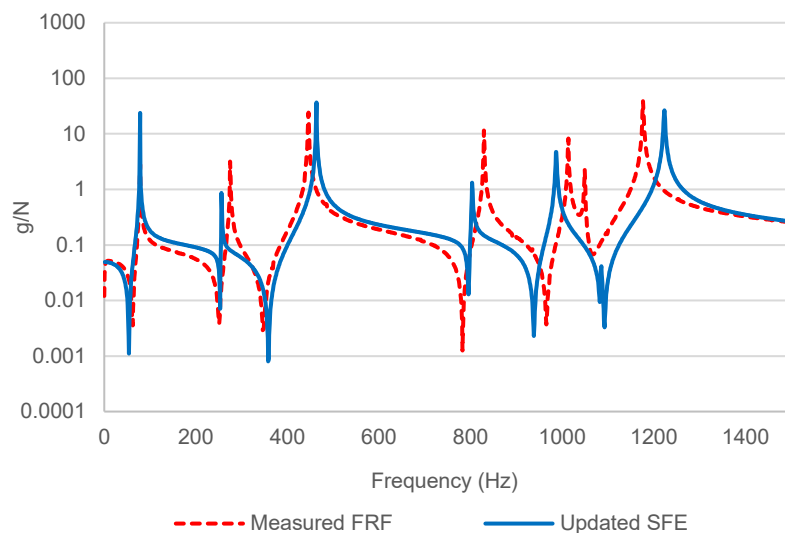


Figure 8. The evaluation of coupled FRF between the test and updated ASFE model at the reference point.

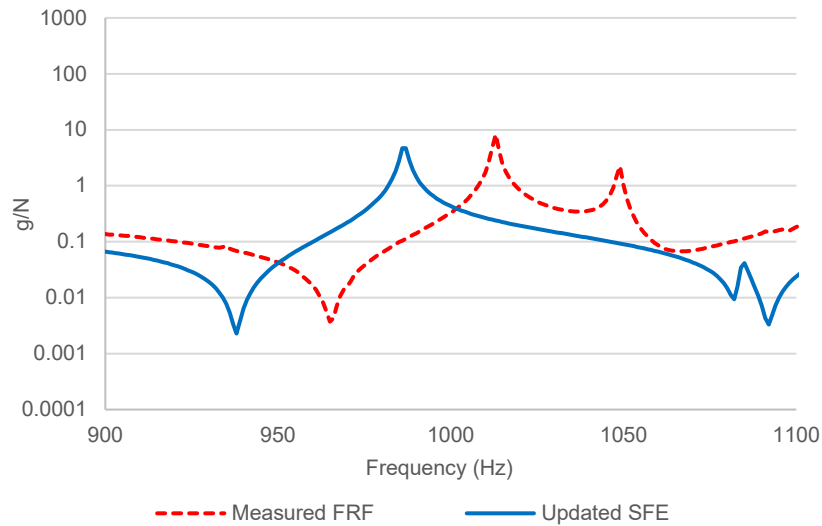


Figure 9. The evaluation of the coupled FRF between the test and updated SFE model at the reference point at a range of 900 to 1100 Hz.

The comparison of the coupled FRFs in Figure 10 shows that the proposed expanded ASFE model is able to estimate the force-excitation and moment-excitation-rotational FRF required for the FBS method. In other words, the expanded ASFE model successfully provides 75% of a complete FRF coupling matrix, which is the crucial element for the accuracy of the FBS method [2], [6], [21]. Note that the coupling interface lost the joint flexibility in the rotational FRFs during the coupling process. Furthermore, the strong correlation from the comparison indicates that the use of the expanded rotational FRFs from the expanded ASFE model in the coupling process significantly improved the accuracy and flexibility of the coupling interfaces of the assembled structure.

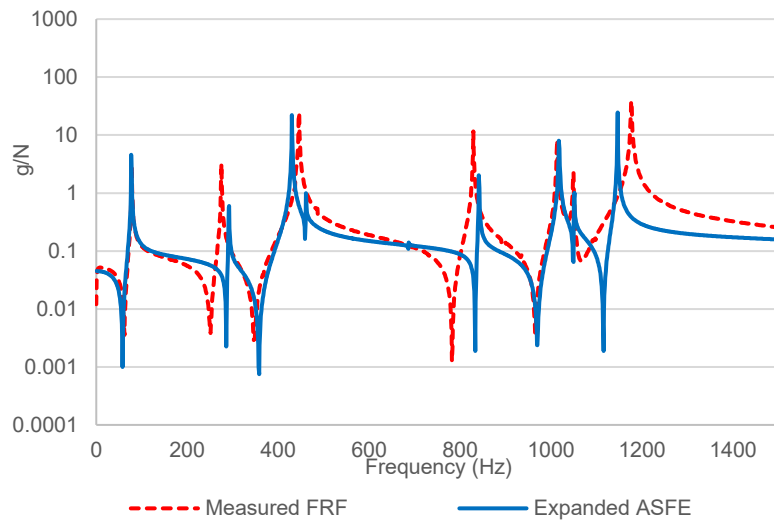


Figure 10. The evaluation of the coupled FRF between the test and expanded ASFE model at the reference point.

Another noteworthy point is that a significant improvement in the correlation between the tested and the predicted coupled FRF is observed within the frequency range of interest from 900 to 1100, as shown in Figure 10. The 6th and 7th resonance peaks show a similar pattern in terms of resonance and anti-resonance of the test FRF.

FRAC analysis was performed to assess the level of correlation between the test and the FBS, using the expanded model of the assembled structure. The value calculated from the analysis is 84.44%, which is significantly higher than the FBS using the updated SFE model. The result indicates a dramatic improvement in the predictive ability of the proposed approach, namely the expanded ASFE model. Thus, the results of this study indicate that the proposed approach provides a more practical and reliable solution for calculating the coupled FRF of the assembled structure compared to the method in [16].

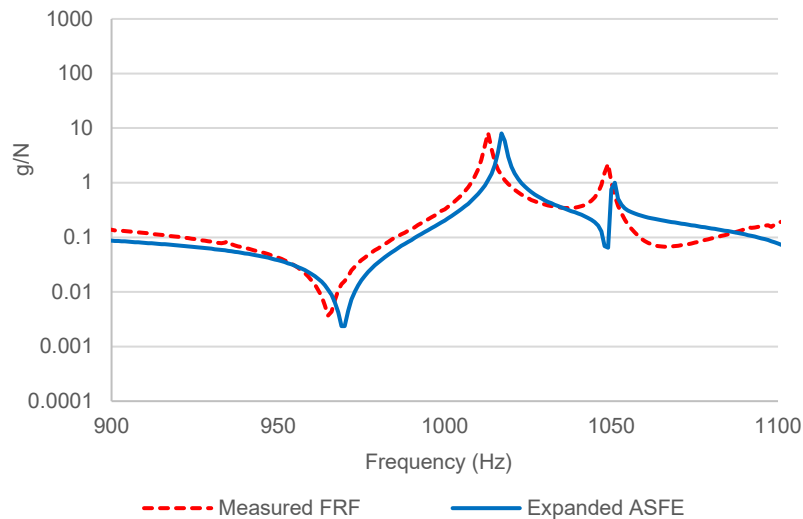


Figure 11. The evaluation of the coupled FRFs at the reference point within the range of 900 to 1100 Hz between test and expanded ASFE model.

CONCLUSION

An alternative approach to obtain a complete coupling matrix including translational and rotational FRFs using the model updating and mode expansion method for the FBS method is presented and discussed. The proposed approach was demonstrated on an irregular plate. It was found that the rotational FRF obtained by the proposed approach agrees well with that obtained by the piezoelectric direct rotational accelerometer. To predict the FRF of the assembled structure, the proposed approach was used in the FBS method by coupling the FRF obtained from the expanded ASFE with the FRF derived from the beam model. A high degree of accuracy was observed when applying the proposed approach to the prediction of the coupled FRF. This approach appears to be effective in accurately estimating the rotational FRF, which is crucial in structural dynamics. The proposed approach can be further improved by performing FRF expansion using System Equivalent Model Mixing (SEMM) and using inaccurate node groups (VIKING) for FRF coupling.

ACKNOWLEDGEMENT

This research has been funded by the Ministry of Higher Education (MOHE) and Universiti Teknologi MARA via Fundamental Research Grant Scheme (FRGS600-IRMI/FRGS 5/3 (335/2019)).

REFERENCES

- [1] M. Law and S. Ihlenfeldt, "A frequency-based substructuring approach to efficiently model position-dependent dynamics in machine tools," *P. I. Mech. Eng. K-J. Mul.*, vol. 229, no. 3, pp. 304–317, 2015, doi: 10.1177/1464419314562264.
- [2] M. Law, H. Rentzsch, and S. Ihlenfeldt, "Predicting mobile machine tool dynamics by experimental dynamic substructuring," *Int. J. Mach. Tools Manuf.*, vol. 108, pp. 127–134, 2016, doi: 10.1016/j.ijmachtools.2016.06.006.
- [3] M. Law, H. Rentzsch, and S. Ihlenfeldt, "Development of a dynamic substructuring framework to facilitate in situ machining solutions using mobile machine tools," *Procedia Manuf.*, vol. 1, pp. 756–767, 2015, doi: 10.1016/j.promfg.2015.09.054.
- [4] G. Čepon, A. Drozg, and M. Boltežar, "Introduction of line contact in frequency-based substructuring process using measured rotational degrees of freedom," *J. Phys. Conf. Ser.*, vol. 1264, p. 012025, 2019, doi: 10.1088/1742-6596/1264/1/012025.
- [5] T. J. Gibbons, E. Öztürk, and N. D. Sims, "Rotational degree-of-freedom synthesis: An optimised finite difference method for non-exact data," *J. Sound Vib.*, vol. 412, pp. 207–221, 2018, doi: 10.1016/j.jsv.2017.09.031.
- [6] A. Drozg, G. Čepon, and M. Boltežar, "Full-degrees-of-freedom frequency based substructuring," *Mech. Syst. Signal Process.*, vol. 98, pp. 570–579, 2018, doi: 10.1016/j.ymsp.2017.04.051.
- [7] S. H. Tsai, H. Ouyang, and J. Y. Chang, "Identification of torsional receptances," *Mech. Syst. Signal Process.*, vol. 126, pp. 116–136, 2019, doi: 10.1016/j.ymsp.2019.01.050.
- [8] M. V. Van Der Seijs, D. De Klerk, and D. J. Rixen, "General framework for transfer path analysis: History, theory and classification of techniques," *Mech. Syst. Signal Process.*, vol. 68–69, no. August, pp. 217–244, 2016, doi: 10.1016/j.ymsp.2015.08.004.
- [9] P. Avitabile and J. O'Callahan, "Frequency response function expansion for unmeasured translation and rotation DOFS for impedance modelling applications," *Mech. Syst. Signal Process.*, vol. 17, no. 4, pp. 723–745, 2003, doi: 10.1006/mssp.2001.1457.
- [10] D. Montalv, "Estimation of the rotational terms of the dynamic response matrix," *Shock. Vib.*, vol. 11, pp. 333–350, 2004, doi: 10.1155/2004/780837.
- [11] J. E. Mottershead, A. Kyprianou, and H. Ouyang, "Structural modification. Part 1: Rotational receptances," *J. Sound Vib.*, vol. 284, no. 1–2, pp. 249–265, 2005, doi: 10.1016/j.jsv.2004.06.021.
- [12] J. E. Mottershead et al., "Structural modification of a helicopter tailcone," *J. Sound Vib.*, vol. 298, no. 1–2, pp. 366–384, 2006, doi: 10.1016/j.jsv.2006.05.026.

- [13] M. Dumont and N. Kinsley, "Rotational accelerometers and their usage in investigating shaker head rotations," *Sensor and Instrumentation*, vol. 5, pp. 85–92, 2016, doi: 10.1007/978-3-319-15212-7_10.
- [14] V. M. Fremd, "Piezoelectric rotational accelerometers," *Seismic Instruments*, vol. 54, no. 3, pp. 293–298, 2018.
- [15] A. Droz, J. Rogelj, G. Čepon, and M. Boltežar, "On the performance of direct piezoelectric rotational accelerometers in experimental structural dynamics," *Meas.: J. Int. Meas. Confed.*, vol. 127, no. February, pp. 292–298, 2018, doi: 10.1016/j.measurement.2018.05.081.
- [16] W. I. I. Wan Iskandar Mirza *et al.*, "The prediction of the dynamic behaviour of a structure using model updating and frequency based substructuring," *IOP Conf. Ser.: Mater. Sci. Eng.*, vol. 506, no. 1, 2019, doi: 10.1088/1757-899X/506/1/012011.
- [17] H. S. Lim and H. H. Yoo, "Modal analysis of a multi-blade system undergoing rotational motion," *J. Mech. Sci.*, vol. 23, no. 8, pp. 2051–2058, 2009, doi: 10.1007/s12206-009-0431-3.
- [18] R. Omar *et al.*, "Finite element modelling and updating for bolted lap joints," *J. Mech. Eng.*, vol. SI 4, no. 3, pp. 202–222, 2017.
- [19] R. Omar *et al.*, "Efficient finite element modelling for the investigation of the dynamic behaviour of a structure with bolted joints," *AIP Conf. Proc.*, vol. 1952, p. 020082, 2018, doi: 10.1063/1.5032044.
- [20] Z. Ming, G. Qintao, Y. Lin, and Z. Baoqiang, "Finite element model updating of jointed structure based on modal and strain frequency response function," *J. Mech. Sci.*, vol. 33, no. 10, pp. 4583–4593, 2019, doi: 10.1007/s12206-019-0902-0.
- [21] M. S. M. Zin *et al.*, "Frequency response function (FRF) based updating of a laser spot welded structure," *AIP Conf. Proc.*, vol. 020055, p. 020055, 2018, doi: 10.1063/1.5032017.
- [22] W. I. . Wan Iskandar Mirza *et al.*, "Reduced order model for model updating of a jointed structure," *J. Eng. Appl. Sci.*, vol. 11, pp. 2383–2386, 2016, doi: 10.3923/jeasci.2016.2383.2386.
- [23] M. Pastor, M. Binda, and T. Harčarik, "Modal assurance criterion," *Procedia Eng.*, vol. 48, pp. 543–548, 2012, doi: 10.1016/j.proeng.2012.09.551.
- [24] D. Lee, T.-S. Ahn, and H.-S. Kim, "A metric on the similarity between two frequency response functions," *J. Sound Vib.*, vol. 436, pp. 32–45, Dec. 2018, doi: 10.1016/j.jsv.2018.08.051.